Nanofiber-Reinforced Polymers Prepared by Fused Deposition Modeling

M. L. Shofner,[1] K. Lozano,[2] F. J. Rodríguez-Macías,[3] E. V. Barrera[1]

[1]*Department of Mechanical Engineering and Materials Science, Rice University, Houston, Texas 77005*
[2]*Department of Engineering, The University of Texas Pan American, Edinburg, Texas 78539*
[3]*Department of Chemistry, Rice University, Houston, Texas 77005*

Received 26 April 2002; accepted 22 December 2002

ABSTRACT: Vapor-grown carbon fibers (VGCFs), a practical model nanofiber for single-walled carbon nanotubes, were combined with an acrylonitrile–butadiene–styrene (ABS) copolymer to create a composite material for use with fused deposition modeling (FDM). Continuous filament feedstock materials were extruded from Banbury mixed composites with a maximum composition of 10 wt % nanofibers. Issues of dispersion, porosity, and fiber alignment were studied. SEM images indicated that the VGCFs were well dispersed and evenly distributed in the matrix and that no porosity existed in the composite material following FDM processing. VGCFs aligned both in the filament feedstock and in the FDM traces suggested that nanofibers, in general, can be aligned through extrusion/shear processing. The feedstock materials were processed into test specimens for mechanical property comparisons with unfilled ABS. The VGCF-filled ABS swelled less than did the plain ABS at similar processing conditions due to the increased stiffness. The tensile strength and modulus of the VGCF-filled ABS increased an average of 39 and 60%, respectively, over the unfilled ABS. Storage modulus measurements from dynamic mechanical analysis indicated that the stiffness increased 68%. The fracture behavior of the composite material indicated that the VGCFs act as restrictions to the chain mobility of the polymer. © 2003 Wiley Periodicals, Inc. J Appl Polym Sci 89: 3081–3090, 2003

Key words: nanocomposites; mechanical properties; viscoelastic properties

INTRODUCTION

Vapor-grown carbon fiber (VGCF)-reinforced polymer composites are of recent interest because of their unique combination of favorable thermal, electrical, and mechanical properties. Superior thermal and electrical properties were reported in previous work with VGCFs in a polypropylene matrix. Mechanical property enhancements were obtained, but further manipulation of the VGCFs through alignment and fiber treatment will be required for optimal enhancements.[1–3] In addition to the multifunctional property improvements provided by VGCFs, their use in polymers is proving to be an effective approach to understanding the processing of single-walled carbon nanotube (SWNT)/polymer composite materials. VGCFs are prepared in a manner similar to SWNTs and are readily available at a relatively low cost.[4–6] Research by Lozano et al.[1–2,4] has led to the knowledge that VGCFs can be mixed through shear processing without fiber breakage and individual fiber dispersion can be achieved starting from a tangled mass. In this research, the processing approach went beyond Banbury mixing to include extrusion and elongational flow to produce well-dispersed, low-porosity feedstock material for fused deposition modeling (FDM).

FDM is a rapid prototyping manufacturing technique (marketed by Stratasys Inc., Eden Prairie, MN) that uses information from a three-dimensional computer-generated model to produce a part. The computer model is sliced into layers, and the information from the model is used to build a part that is constructed layer by layer on top of a removable support material. The process uses continuous filament feedstock as its base material. The feedstock is extruded through a heated nozzle moving in the *X*–*Y* plane. Once the machine has completed a layer of the part, the machine stage lowers in the *Z* direction to build the next layer above the layer just finished. This technology allows for the manufacture of parts with complex shapes, models on demand, and molds. Its compact size and feedstock material also enable FDM with remote manufacturing capabilities.[7,8]

A number of feedstock materials are available for FDM, including an investment casting wax, thermo-

Correspondence to: E. V. Barrera (ebarrera@rice.edu).
Contract grant sponsor: NASA; contract grant numbers: NGT9-23; NCC9-77.
Contract grant sponsor: NSF; contract grant numbers: CMS0092621; CMS0078990.
Contract grant sponsor: NSF Graduate Fellowship Program.

Journal of Applied Polymer Science, Vol. 89, 3081–3090 (2003)

plastic polyester-based elastomer, poly(acrylonitrile–butadiene–styrene) (ABS) copolymer, polycarbonate, and polyphenylsulfone.[9] Most of these materials do not possess the strength to produce fully functional parts using FDM, restricting the use of FDM and other rapid prototyping techniques. The development of new materials for FDM is a way to overcome this limitation and extend its application range. In addition to intrinsically stronger materials such as ceramics and metal, reinforced polymers are being successfully developed with discontinuous fibers.[10,11] These materials have shown initial gains in tensile strength and interlayer strength, often the weak link in an FDM part. In particular, nanofiber polymer composites are perceived as materials that should significantly enhance FDM, selective laser sintering (SLS), and other rapid prototyping methods because of their unique multifunctional properties (i.e., structural/electrical, structural/thermal, and structural/impact).

ABS was chosen for this research because it produces high-strength parts compared to other FDM materials, and it is compatible with all FDM systems. Continuous filament materials were produced using pelletized VGCFs in ABS. Pelletized, in this case, refers to a processing method in which a latex sizing is placed on the nanofibers to improve handling. FDM parts were produced including tensile test specimens of different sizes. Parts were also made connecting plain ABS to the VGCF composite, demonstrating that the new materials can work in conjunction with the currently available ABS and that composition gradients are possible. In this study, the compatibility of nanofiber/polymer matrix composites with the FDM process was evaluated, dynamic mechanical analysis and tensile tests were conducted, and the fractured regions of the samples were analyzed using scanning electron microscopy. Fractography was used to verify the absence of porosity and homogeneous fiber dispersion. Also, fractography of the fractured surfaces was used to verify the presence of aligned nanofibers in the filament feedstock and FDM parts. X-ray diffraction, Raman spectroscopy, and electrical resistivity measurements were also made to evaluate alignment, but sample conditions hindered the data collection. The property improvements observed demonstrated that these composite materials enhance the use of rapid prototyping techniques, such as FDM.

BACKGROUND

VGCFs in polymer composites

VGCFs are known to exhibit high stiffness and strength. The combination of high strength, low weight, and high aspect ratio distinguishes them from other types of carbon fibers and reinforcements.[12,13] These favorable properties make them attractive for use in polymer matrix composites. Experimental results from previously published research efforts indicate that VGCFs are suitable reinforcing agents for polymers. Lozano and Barrera demonstrated a 100% increase in the dynamic mechanical properties with only 2 wt % VGCF in a polypropylene matrix.[1] Other work by Tibbetts and McHugh, with a higher loading of VGCFs in polypropylene, produced 200 and 400% increases in the tensile strength and modulus, respectively, through postprocessing treatment of the VGCFs.[14] Patton et al. combined VGCFs with an epoxy and poly(phenylene sulfide) to improve the flexural properties of the matrix materials. They obtained 68 and 91% increases in the flexural strength in epoxy and poly(phenylene sulfide), respectively, with a nominal fiber loading of 20% by volume.[15]

The first step in the development of nanofiber-reinforced polymer composites was the removal of amorphous carbon particles and catalysts from nanofiber production. Purification of VGCFs was accomplished previously but continues to be studied so that high-volume and low-costs methods can be established.[4,16] Fiber functionalization is considered the next improvement to nanofiber-reinforced composites. Functionalization promotes different bonding interactions with the selected matrix to enhance shear transfer interactions. Lozano et al.[4] purified and functionalized VGCFs where hydroxyl and carboxyl groups resulted along with hydrocarbons and quinone structural attachments. Also, Glasgow et al.[17] modified the surfaces of VGCFs using air etching and CO_2 etching to successfully improve fiber–matrix adhesion. Aside from fiber preparation, processing was a key step in the development of these composites. The size of VGCFs gives them a specific advantage in compounding and molding. They can be processed by conventional plastic technologies that use high shear without sustaining damage. Homogeneous dispersion of VGCFs has been achieved in this manner as reported by Lozano et al.[1,2] Other works have produced segregated dispersions of nanofibers for electrical applications, in part, because the tangled masses of nanofibers could not be dispersed.[18,19]

One of the most promising near-term uses of VGCF-reinforced composites is in electrostatic dissipating (ESD) materials, commonly used for electronics packaging. Values of electrical resistivity in the ESD range are achieved with VGCF concentrations higher than 12 wt % without compromising the processing viscosity or reducing the mechanical strength of the polymer matrix.[2] To produce enhancements in mechanical properties at even lower concentrations of reinforcements, research is being conducted concerning alignment of the nanofibers within the polymer matrix. Achieving alignment will further promote the appli-

cation of nanofiber-reinforced polymer composites as multifunctional materials.[3]

Filled feedstock materials for FDM

Filled feedstock for FDM is a topic of much active research. The majority of this work concerns the production of functional ceramic parts. Ceramic particles are combined with a polymeric binder to create the feedstock. The parts produced from this material are subjected to binder burnout cycles. Then, they are infiltrated with another material, sintered to densify the ceramic part, or considered finished. The concepts used to create functional ceramic parts with FDM could be used to remove the polymer matrix surrounding nanofibers such as VGCFs and SWNTs to create a part consisting of only nanofibers or a nanofiber template to be infiltrated with another material.[1] Novel piezoelectric ceramic/polymer composite materials, functional ceramic materials, and porous ceramic biomaterials have been produced in this manner.[20–23] A part of the research to produce these ceramic-filled feedstock materials has been focused on achieving dispersion and controlling viscosity to achieve uniform dispersion of the ceramic particles in the polymer binder.[20–25] These investigations are useful and relevant to the current research because issues of viscosity and dispersion were crucial to their success.

Fiber-reinforced polymers for direct use with FDM is a less active research topic. As with ceramic-filled feedstock materials, homogeneous dispersion of reinforcements and melt viscosity are crucial to the integration of these materials into FDM processing. Two polymer matrix composite materials previously studied in this regard are glass fiber in ABS and thermotropic liquid crystal polymer (TLCP) fibril-reinforced polypropylene.[10,11] With the glass fiber-reinforced materials, the researchers found that the addition of fibers to the ABS reduced the flexibility of the material to an extent that it could not be used with the FDM process. The addition of a plasticizer and compatibilizer to the glass fiber/ABS composite facilitated its use with FDM and produced gains in longitudinal mechanical properties and even larger increases in interlayer strength. The TLCP fibril-reinforced material also produced substantial increases in the modulus with respect to polypropylene and ABS in a preliminary study. In addition to improved mechanical properties, both materials showed some preferential orientation of the fibers following processing by FDM. The alignment of fibers through FDM is a desirable outcome with nanofiber-filled polymers. To obtain enhanced mechanical, electrical, and thermal properties in these composite materials, the fibers should have a high degree of alignment as dictated by their high aspect ratios.

TABLE I
Magnum 213 and Stratasys P400 ABS Properties[26,27]

Property	MAGNUM® 213 ABS	Stratasys P400 ABS
Density (g/cm^3)	1.04	1.05
Tensile strength (MPa)	34.5	34.5
Tensile modulus (GPa)	2.48	2.48
Hardness (Rockwell R)	105	105
Softening point (°C)	104	104

EXPERIMENTAL

Materials

Applied Science, Inc. (Cedarville, OH) supplied VGCFs for this research, known by the trade name Pyrograf III. The VGCFs were provided in pelletized form. The fibers were produced from the catalytic pyrolysis of a hydrocarbon gas, and the structure of the finished fiber consisted of graphene planes oriented around the fiber axis. These fibers had an average diameter of 100 nm and lengths on the order of 100 μm. The VGCFs were combined with a commercially available ABS to create the composite material. As mentioned previously, ABS was chosen from the polymers available for use with FDM because it was able to produce relatively strong parts and ABS was compatible with all Stratasys FDM technologies. The brand of ABS selected for this research was MAGNUM® 213 ABS from Dow Chemical Company (Midland, MI). The ABS was chosen because it has similar physical properties to the P400 ABS marketed by Stratasys Inc. and is available in pellet form.[26,27] A comparison of the two ABS materials is shown in Table I.

Sample preparation

Banbury mixing, compression molding, and extrusion were used to process the composite feedstock for FDM. The Banbury mixing was conducted in a HAAKE Polylab System using a 30-g mixing bowl. ABS was compounded with the VGCFs at high shear rates to achieve a homogeneous dispersion and distribution of fibers in the matrix.[3] A composition of 10 wt % VGCFs was prepared. The mixed material was compression-molded using a heated press, and the resulting sheets were granulated to form the starting material for filament extrusion. The granules were fed into a single-screw extruder and extruded at a rate of 5 rpm. The VGCF/ABS composite feedstock was spooled by hand onto an FDM reel while maintaining a constant filament diameter for the length of the extruded filament. The composite granules were preceded and followed by unfilled ABS pellets to enable recovery of all the VGCFs and reduce the amount of composite material needed to fill the extruder barrel. Consequently, the composition of the feedstock varied

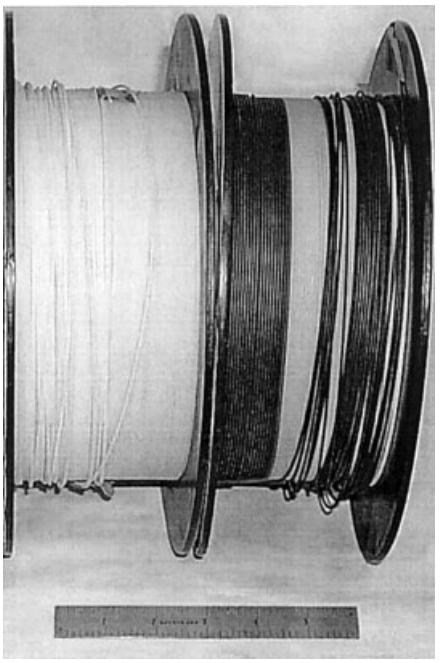

Figure 1 Spools of continuous filament feedstock for FDM. The compositions of these materials from left to right: unfilled ABS and 10 wt % VGCFs in ABS.

over the length of the filament with the maximum composition of 10 wt % VGCFs at the middle of the extrusion run. This approach caused an unexpected morphology in the feedstock at the beginning and end of the run. ABS segregated to the core of the filament surrounded by a layer of VGCF/ABS composite material. The segregation disappeared as the VGCF concentration increased to a maximum. A spool of unfilled ABS was also extruded from the plain pellets to use as a baseline material. Each filament had a nominal diameter of 1.7 mm to facilitate FDM processing. Some variation in the feedstock diameter resulted from manual material collection. Figure 1 shows the spools of unfilled ABS and ABS with VGCFs with approximately 20 m of feedstock on each spool.

The filament feedstock produced from the VGCF/ABS composite was less flexible in nature than was the unfilled ABS, but it could be collected on FDM spools and processed. The prepared spools were used in a Stratasys FDM 1600 Modeler. Several different parts were made including dome shapes, spacecraft models, logos, and tensile tests samples, as shown in Figure 2. Unfilled ABS and VGCF/ABS materials were used to fabricate straight-bar and two types of dogbone tensile samples for the mechanical property measurements with different layer orientations as described in Table II. In this research, an orientation of 0° indicated that the extruded road is parallel to the long axis of the sample and testing direction. Conversely, an orientation of 90° indicated that the extruded road is perpendicular to the long axis of the part and testing direction. The straight-bar samples had 11 layers, and the samples had layer orientations of 0°/90°, 90°/0°, and 45°/45°. The first angle indicates the alignment of the top layer (last built), so in the case of the 0°/90° samples, six layers were parallel to the long axis of the part. The second set of samples manufactured had a dogbone shape and six layers. The shape was similar to an ASTM D638 Type V specimen but with a slightly wider gauge section. The layers of these specimens were oriented in a 10°/90° arrangement. The second set of dogbone samples was made to the Type V geometry outlined by ASTM D638, and all five layers of these specimens were oriented parallel to the long axis of the part. This set of samples also contained tensile samples made from the Stratasys P400 ABS for comparison. Whereas the first two sets of samples were made using the default build parameters, the Type V specimens were made using optimized build parameters to maximize the strength of the parts. Work by Rodriguez et al. has led to an increased understanding of the relationship between build parameters and properties for the Stratasys P400 ABS.[28–30] The parameters for the P400 ABS and MAGNUM® samples were set according to a previous work by Rodriguez et al.[28] The build parameters for the-filled samples were adjusted slightly to accommodate the reduced swelling of the filled feedstock.

Analysis

Tensile tests were conducted using an MTS 858 Mini Bionix Testing System with a 10-kN load cell. Tests were conducted based on the ASTM D638 standard at a test speed of 25.4 mm/min. Tensile strength values were calculated from the highest load experienced

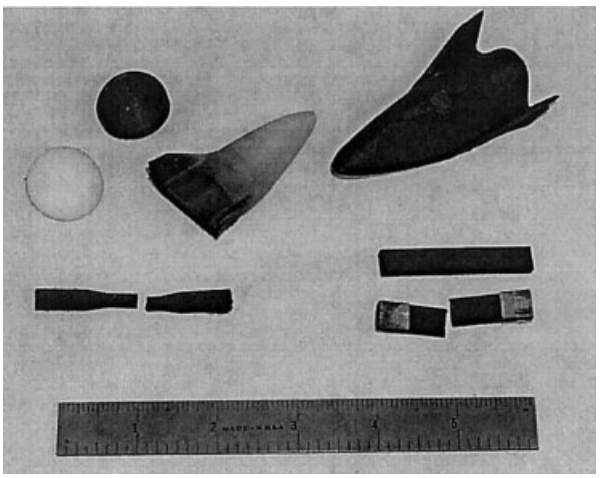

Figure 2 X38 replicas, domes, and tensile test specimens made from VGCF/ABS composite and unfilled ABS. Note that the smaller X38 model shows a graded interface from composite to unfilled ABS, indicating the compatibility of the two materials.

TABLE II
Tensile Test Specimen Details

Sample set	Sample shape	Nominal dimensions (mm)	Materials	Layer orientation	No. samples
1	Straight bar	9.4 (width)	MAGNUM® ABS	0°/90°	4
		3 (thickness)	VGCF in MAGNUM® ABS	0°/90°	4
		51 (overall length)		90°/0°	4
				45°/45°	7
2	Dogbone	4.8 (width)	MAGNUM® ABS	10°/90°	12
		1.6 (thickness)	VGCF in MAGNUM® ABS	10°/90°	12
		12.7 (gauge length)			
3	ASTM D638	3.2 (width)	P400 ABS	0°/0°	9
	Type V	1.3 (thickness)	MAGNUM® ABS	0°/0°	8
	Dogbone	7.6 (gauge length)	VGCF in MAGNUM® ABS	0°/0°	6

during testing and the original cross-sectional area of the part. Tensile modulus measurements were taken from the initial slope of the stress/strain curve. The straight-bar samples and the Type V dogbones were tested with plastic tabs adhered onto the ends of the test specimen, and the 10°/90° dogbone specimens were put into direct contact with the grips. Care was taken in the placement and orientation of the samples to better understand effects that might be associated with the orientation of the FDM build process (top and bottom orientations) and positioning of the samples in the grips.

The fracture surfaces of tensile specimens and the cross sections of continuous filaments were analyzed with a Phillips Electroscan XL30 scanning electron microscope (SEM). The samples were coated with gold even though a concentration of 10 wt % VGCFs lowered the electrical resistivity of the material, preventing charging by the electron beam.[3] The morphology of the tensile specimen fracture surfaces was studied for changes in the failure nature of the composite material with respect to the unfilled ABS and nanofiber alignment. The cross sections of the filaments were also analyzed for alignment.[16,31]

After tensile testing, some of the material from the second sample set was fashioned into a thin sheet using heated compression molding. The traces of material were oriented along the long axis of the sample before compression molding, but the sample preparation method may have decreased the degree of fiber alignment. Rectangular-shaped samples with nominal cross-sectional dimensions of 12 × 1.5 mm were cut from the sheet and tested using dynamic mechanical analysis (DMA) to corroborate the reinforced materials' tensile test results. The equipment used was a 2980 DMA from TA Instruments. The tests were performed in single-cantilever mode at a frequency of 1 Hz. The samples were heated from 40 to 90°C at a rate of 5°C per min.

RESULTS AND DISCUSSION

VGCF dispersion and alignment

VGCF dispersion and alignment was observed in the feedstock material and the fractured tensile specimens using SEM. Figure 3(a) shows the tangled mass of VGCFs prior to mixing, and Figure 3(b) shows the

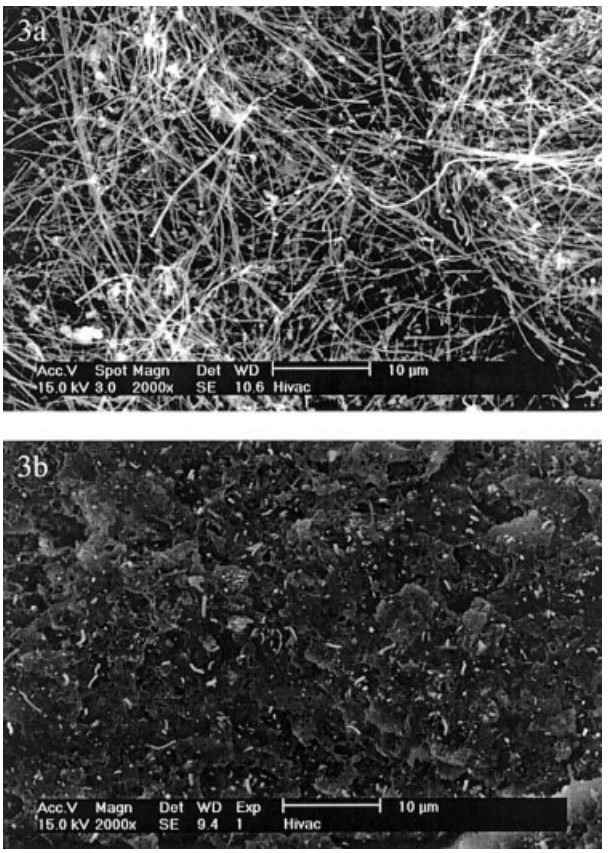

Figure 3 SEM images of the VGCFs before and after materials processing. Image (a) shows the tangled mass of fibers prior to mixing. Image (b) shows the composite material following mixing and extrusion. Homogeneous dispersion and individual fiber separation were achieved in the starting material for FDM.

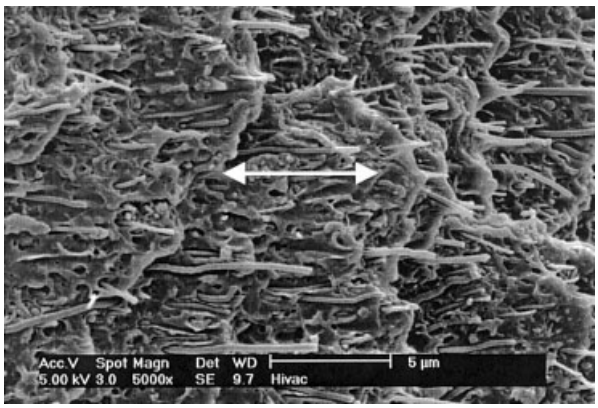

Figure 4 FDM feedstock surface in the longitudinal direction. The exposed surface shows a high degree of VGCF alignment and aspects of poor wetting conditions.[16]

even dispersion and distribution of the VGCFs in the feedstock material after Banbury mixing and extrusion. The image shows all the fibers surrounded by the polymer matrix and isolated from each other. Figure 4 demonstrates the degree of alignment obtained in the feedstock material. The VGCFs are highly aligned with respect to the axial direction of the extrusion as indicated by the arrow. In addition to alignment, Figure 4 shows the level of interaction between the VGCFs and the ABS. The wetting appears to be poor since the surfaces of the fibers appear clean and the polymer is not highly deformed around the fibers. The poor fiber/matrix adhesion creates a low level of resistance to fiber pullout. The fibers that pulled out of the matrix were undamaged from the high shear that occurs in the mixing and extrusion processes because they possess lengths similar to the starting conditions. Preferential fiber orientation produced an improvement in strength unlike previous work with isotropic samples that showed no strength improvement.[2]

Figure 5 shows the fracture surfaces of the extruded paths in a 10°/90° tensile sample. Images 5(a,b) are the 10° and 90° layers, respectively. The fibers rotated 10° from the testing direction [Fig. 5(a)] appear significantly shorter than those aligned perpendicular to the testing direction. This indicates that the fibers more closely aligned to the testing direction take the load, consistent with an isostrain condition, and subsequently break. The layers in Figure 5(b) were loaded in an isostress condition and experienced failure from low normal stress. These images demonstrate similar alignment conditions and fiber dispersion to Figures 3 and 4. Poor wetting is also evident from the appearance of troughs around the VGCFs. The micron-size circular particles are the segregated butadiene phase of the ABS. These features were also observed in the unfilled ABS. Figure 6 is the boundary between two layers of the 10°/90° tensile sample. This image combines the aspects of Figure 5(a,b). It further shows the

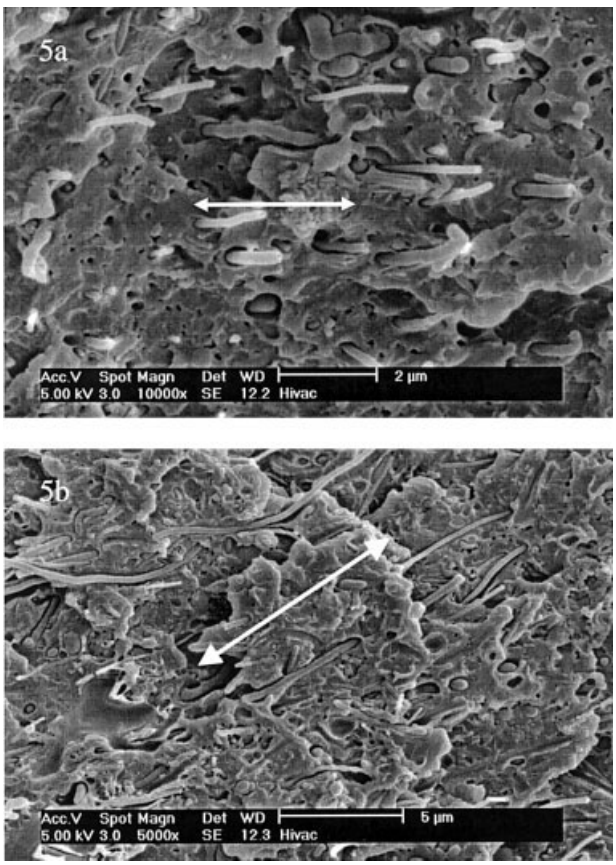

Figure 5 SEM images of extruded path fracture surfaces. Images (a,b) display paths aligned approximately parallel and perpendicular to the applied load, respectively. In both images, the VGCFs are aligned in the direction of extrusion during FDM processing.

degree of alignment with the direction of the extruded paths. The holes seen on the sample surfaces are produced from VGCF pullout and not from process porosity. Process porosity tended to show surface morphological differences in the polymer and was only observed in a few of the early processed samples.

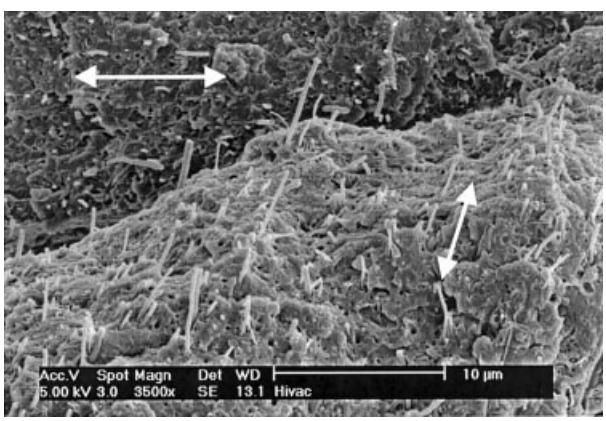

Figure 6 SEM image of the boundary between two extruded paths from adjacent layers. As with Figure 5, the VGCFs are aligned with respect to the extrusion direction.

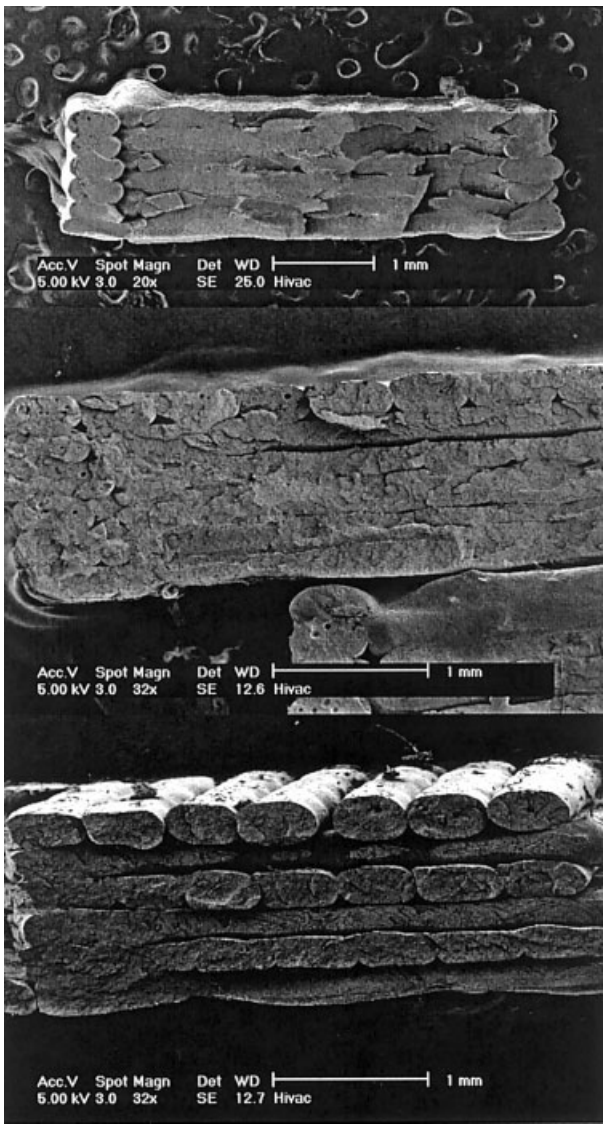

Figure 7 Fracture surfaces of tensile test specimens from sample set 2. These images show varying degrees of fusion between the layers and individual FDM traces. The top image is unfilled ABS. The middle and bottom images are VGCF/ABS. Less swelling of the composite material and variations in the feedstock diameter led to inconsistent fusion of the layers.

Mechanical properties

All three sets of tensile specimens showed that the VGCF/ABS composite had increased tensile strength with respect to the unfilled ABS. However, the composite specimens also showed a drastic decrease in elongation to failure as the fracture mode changed from ductile to brittle. The brittle behavior resulted from low resistance to fiber pullout and decreased interlayer fusion. Shown in Figure 7 are samples with six layers, arranged in the 10°/90° pattern. Observation of the fracture surfaces for straight-bar and dogbone samples of the unfilled ABS showed consistent results of relatively good fusion through the cross section of the specimen. All specimens with VGCFs possessed decreased interlayer fusion with respect to the unfilled samples, but the level of interlayer fusion varied between sample sets due to small variations in the feedstock diameter. Since the material was spooled manually, variations were expected. Limited porosity was observed in the VGCF/ABS filament material resulting from the different size distributions of the ABS pellets and the VGCF/ABS pellet granules used during the extrusion process and not from the initial Banbury mixing. Eliminating the unfilled ABS pellets before and after the VGCF/ABS granules during extrusion should remove the porosity from future work.

The straight-bar tensile samples did not effectively measure the strength of the materials because all the samples fractured at the grips, but they were interesting from the standpoint of layer alignment. While the unfilled ABS samples showed a relatively consistent tensile strength, the VGCF/ABS samples had more significant scatter in the data. The error can be attributed to the reduced interlayer fusion. Of the three-part build strategies, the 45°/45° showed the highest increase in tensile strength with an average improvement of 15%. By skewing the layer orientation with respect to the testing direction, fewer intralayer voids occurred in the cross section of the part. The decreased void density resulted in a stronger part. These lessons learned were carried over to the next set of tensile specimens.

In an effort to more effectively measure the materials' tensile strength, the second set of tensile samples was made in a dogbone shape. These samples had a layer stacking sequence of 10°/90°. The top layer was slightly skewed to reduce the intralayer void density while aligning the fibers close to the testing direction. The fracture surfaces of these parts shown in Figure 7 demonstrate an improvement, but it was not consistent. The majority of these samples fractured in the gauge length, and the test results obtained are shown in Figure 8 along with those of the third sample set. The error in the data was larger than that of the straight-bar samples, and the unfilled ABS samples showed a lower spread in the data with respect to the filled samples. The persisting trend indicated that the interlayer fusion in the VGCF/ABS samples was worse than was the interlayer fusion in the ABS samples. Despite the reduced fusion, the VGCF/ABS samples possessed an average tensile strength of 24.4 MPa, 29% higher than that of the unfilled ABS.

To improve the levels of interlayer and intralayer fusion and maximize the part strength, a third set of tensile samples were fabricated using optimized build parameters.[28] Three materials were used to make this set of samples: P400 ABS from Stratasys, MAGNUM® ABS, and VGCF/MAGNUM® ABS. The P400 ABS was added to evaluate the practical similarity of MAGNUM® and P400. These samples had higher tensile

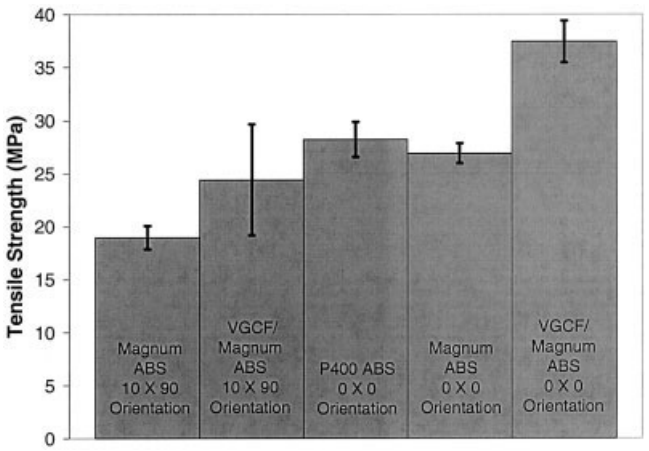

Figure 8 Bar graph of tensile test results from both sets of dogbone specimens. In both sample sets, the VGCF/ABS specimens produced a higher tensile strength. The use of optimized build parameters in sample set 3 increased the strength of the unfilled ABS and VGCF/ABS parts and reduced the scatter in the data for the VGCF/ABS test specimens. The error bars indicate 1 standard deviation.

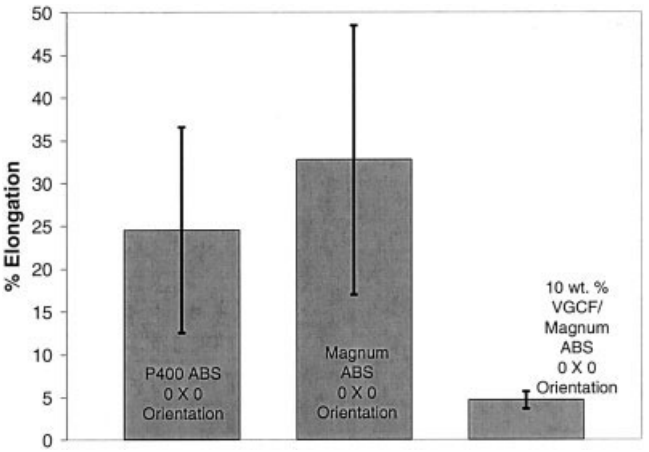

Figure 9 Bar graph of percent elongation to failure results from sample set 3. The addition of VGCFs to the ABS changed the nature of the material from ductile to brittle. Further fiber treatment could result in a less dramatic shift in material behavior. The error bars indicate 1 standard deviation.

strengths as compared to the straight-bar and other dogbone specimens and less scatter in the data of the filled samples. Figure 8 and Table III show the test results for the tensile strength and tensile modulus. The two ABS materials tested similarly. Their average tensile strength and modulus differed by only 1.3 MPa (5%) and 10 MPa (2%), respectively. As with the previous two sets of data, the VGCF/ABS material had an increased tensile strength. The VGCF/ABS composite displayed an average strength of 37.4 MPa and an average modulus of 0.79 GPa, representing respective increases of 39 and 60% with respect to the unfilled ABS tensile samples of the same shape. This result compares favorably when compared to other types of reinforcements studied with FDM. Previous work with glass fiber showed an increase of 19% in the tensile strength at a similar concentration. A compatibilizer was required to obtain further property increases in the glass fiber/ABS composite.[11]

Although the strength of the composite material was larger than its unfilled counterpart, the ductility of the composite material was severely reduced. The brittleness of the composite resulted from poor fiber/matrix bonding and decreased interlayer bonding. Figure 9 shows the elongation-to-failure data for the third set of tensile specimens. The data for both types of unfilled ABS varied over a large range. The VGCF/ABS material was more consistent, but it fractured at a lower level of strain. On average, the elongation to failure decreased 86% with respect to the unfilled ABS. Further postprocessing treatment of the VGCF could improve the ductility of the fibers and, concomitantly, the ductility of the composite. The conferred effect of the nanofibers on the fracture behavior of ABS was similar to the fracture behavior of tightly crosslinked resins where the molecular network was unable to deform sufficiently. In this case, the nanofibers decreased the resistance to yield, acting as constraints for chain mobility. The decrease in chain mobility increased the stiffness of the material that was first observed by the reduction in swelling on the extrusion process. The toughness of the composite was therefore lower than that of the pure ABS but the strength and rigidity were improved.

The experimental results obtained in this work compare well to other published experimental results, but the mechanical measurements do not coincide with those predicted by the rule of mixtures. As the name suggests, the rule-of-mixtures calculation predicts the strength of the composite materials as the sum of the property values of each component multiplied by its volume fraction. Using the tensile strength and mod-

TABLE III
Tensile Test Results for Sample Set 3 (ASTM D638 Type V Specimens)

Material	Tensile strength (MPa)	Standard deviation (MPa)	Tensile modulus (GPa)	Standard deviation (GPa)
P400 ABS	28.2	1.7	0.50	0.03
MAGNUM® ABS	26.9	0.9	0.49	0.03
VGCF/MAGNUM® ABS	37.4	2.0	0.79	0.08

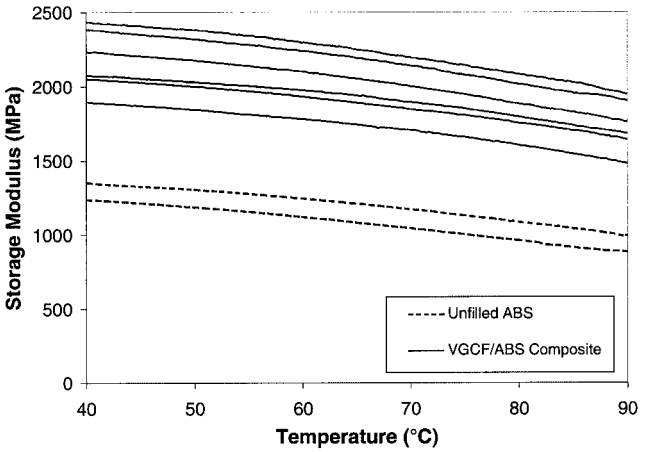

Figure 10 Storage modulus data from DMA tests. The VGCF/ABS composite material showed an average increase of 68%. The other properties measured in this testing, loss modulus and tan delta, did not experience appreciable changes with respect to the unfilled material.

ulus measurements from sample set 3 for the ABS and the tensile strength and modulus values from previously published data for the VGCFs,[5] the composite material should have a tensile strength and modulus of approximately 200 MPa and 24 GPa, respectively. These values are, respectively, one and two orders of magnitude larger than the experimental results. Rule-of-mixtures models generally give higher than reasonable results for discontinuously reinforced composites because they are designed for continuously reinforced composites with an ideal fiber/matrix interface, but the magnitude of the discrepancy indicates that load transfer between the matrix and the fiber is not occurring to an appreciable extent. From the SEM images taken of these materials, the level of wetting is poor between the VGCFs and the ABS interface, indicating that the degree of load transfer is not optimized.

As with the tensile tests, the DMA results indicate an increase in the mechanical properties. Two unfilled samples and six filled samples were tested using the procedure described previously. The VGCF-reinforced ABS possessed a storage modulus 68% greater, on average, than that of the unfilled ABS at 40°C, as shown in Figure 10. The results cannot be directly correlated to the tensile results for two reasons: First, the samples used to make the DMA samples had three layers oriented perpendicular to the long axis of the part, so only one-half of the fibers could be aligned. Second, heated compression molding possibly compromised the degree of fiber alignment, but this increased value for the storage modulus corroborates the increased stiffness obtained in the tensile tests. Also, in this testing, the values of the loss modulus and tan delta were not found to change appreciably.

CONCLUSIONS

Homogeneous composite material consisting of aligned VGCFs in an ABS matrix was processed using Banbury mixing, extrusion, and FDM. The composite material was of good quality as evidenced by high dispersion and distribution of fibers in the matrix and minimal porosity. Mechanical property improvements were observed in the composite material using uniaxial tensile testing and dynamic mechanical analysis. The amount of mechanical property improvement in the tensile tests varied with the build parameters of the sample and the degree of intralayer and interlayer fusion. The results of the tensile tests and the dynamic mechanical analysis indicated that the VGCFs provide additional stiffness and strength while not appreciably affecting the viscous response of the ABS. These test results demonstrated that the VGCFs change the fracture mode of the ABS polymer from ductile to brittle because the bonding between part layers and at the fiber/matrix interface is not ideal. The fracture behavior also indicated that the improved stiffness resulted from the increased resistance to chain mobility in the polymer caused by the addition of VGCFs. FDM process optimization and further fiber treatment to promote better fiber/matrix adhesion could increase the ductility of the composite material and lead to larger mechanical property increases.

The researchers wish to thank Dr. Bradley Files, Dan Petersen, Bonnie Tureaud, and Steve Miller at the NASA Johnson Space Center, Houston, TX, for their assistance with the FDM processing. The authors are also grateful to Applied Sciences, Inc., for providing the VGCFs used in this work. Finally, the authors thank Mary Carmen Villarreal for her assistance with the DMA measurements. This research was funded by NASA (Grants NGT9-23 and NCC9-77), NSF (Grants CMS 0092621 and CMS0078990), and the NSF Graduate Fellowship Program.

References

1. Lozano, K.; Barrera, E. V. J Appl Polym Sci 2001, 79, 125.
2. Lozano, K.; Bonilla-Rios, J.; Barrera, E. V. J Appl Polym Sci 2001, 80, 1162.
3. Lozano, K. JOM 2000, 11, 34.
4. Lozano, K.; Files, B.; Rodríguez-Macías, F. J.; Barrera, E. V. In TMS Fall Meeting Proceedings, 1999; Powder Materials: Current Research and Industrial Practice; p 333.
5. Tibbetts, G. G. Carbon 1989, 27, 745.
6. http://www.fibrils.com/Techpage.htm.
7. Crump, S. S. U.S. Patent 5 121 329, 1992.
8. Walters, W. A. In Solid Freeform Fabrication Symposium Proceedings, 1992; p 301.
9. http://www.stratasys.com.
10. Gray IV, R. W.; Baird, D. G.; Bøhn, J. H. Rapid Prototyp J 1998, 4, 14.
11. Zhong, W.; Li, F.; Zhang, Z.; Song, L.; Li, Z. Mater Sci Eng A 2001, 301, 125.
12. Jacobsen, R. L.; Tritt, T. M.; Guth, J. R.; Ehrlich, A. C.; Gillespie, D. J. Carbon 1995, 33, 1217.

13. Grande, J. A. Mod Plast 1996, 73, 41.
14. Tibbetts, G. G.; McHugh, J. J. J Mater Res 1999, 14, 2871.
15. Pittman, C. U., Jr.; Patton, R. D.; Wang, L.; Hill, J. R. Compos Part A Appl Sci Manuf 1999, 30, 1081.
16. Barrera, E. V. JOM 2000, 11, 38.
17. Glasgow, D. G.; Lake, M. L.; Tibbetts, G. G.; Finegan, J. C.; Kwag, C. In SAMPE-ACCE-DOE Advanced Materials Conference Proceedings: Planes, Trains, Automobiles . . . and Bridges, Too, 1999; p 156.
18. Sandler, J.; Shaffer, M. S. P.; Prasse, T.; Bauhofer, W.; Schulte, K.; Windle, A. H. Polymer 1999, 40, 5967.
19. Friend, S. O.; Barber, J. J. U.S. Patent 5 611 964, 1997.
20. Lous, G. M.; Cornejo, I. A.; McNulty, T. F.; Safari, A.; Danforth, S. C. In Materials Research Society Symposium Proceedings, 1999, 542, 105.
21. Gasdaska, C. J.; Clancy, R.; Jamalabad, V.; Dalfonzo, D. In Materials Research Society Symposium, Proceedings, 1999, 542, 79.
22. Rangarajan, S.; Harper, B.; McCuiston, R.; Safari, A.; Kalman, Z.; Mayo, W.; Danforth, S. C.; Gasdaska, C. In Materials Research Society Symposium Proceedings, 2000, 625, 179.
23. Cornejo, I. A.; McNulty, T. F.; Lee, S.; Bianchi, E.; Danforth, S. C.; Safari, A.; TenHuisen, K. S.; Janas, V. F. Ceram Trans 2000, 110, 183.
24. Lombardi, J. L.; Hoffman, R. A.; Waters, J. A.; Popovich, D.; Souvignier, C.; Boggavarapu, S. In Solid Freeform Fabrication Symposium Proceedings, 1997; p 457.
25. Venkataraman, N.; Rangarajan, S.; Matthewson, M. J.; Harper, B.; Safari, A.; Danforth, S. C.; Wu, G.; Langrana, N.; Guceri, S.; Yardimci, A. Rapid Prototyp J 2000, 6, 244.
26. http://www.prototype3d.com/html/techsheets/data.html.
27. http://www.matweb.com/SpecificMaterial.asp?bassnum=PDW073&group=General.
28. Rodriguez, J. F.; Thomas, J. P.; Renaud, J. E. In Solid Freeform Fabrication Symposium Proceedings, 1999; p 335.
29. Rodriguez, J. F.; Thomas, J. P.; Renaud, J. E. In ASME Design Engineering Technical Conferences Proceedings, 2000; p 1.
30. Rodriguez, J. F.; Thomas, J. P.; Renaud, J. E. Rapid Prototyp J 2000, 6, 175.
31. Ajayan, P. M.; Stephan, O.; Colliex, C.; Trauth, D. Science 1994, 265, 1212.